Artificial Intelligence in Geosciences 6 (2025) 100150

Contents lists available at ScienceDirect

Artificial Intelligence in Geosciences

journal homepage: www.keaipublishing.com/en/journals/artificial-intelligence-in-geosciences

Machine learning applied to recognition of dinoflagellate cysts: Type study with the species *Batioladinium longicornutum*

A. Sanches [a,b], B. Ağbulut [c,e], L. Castro [b,d], M. Vieira [b,f,*]

[a] Rockrose, Lda, Rua da Igreja, 29, 7750-338, Mértola, Portugal
[b] GeoBioTec - polo FCT, NOVA School of Science and Technology, Campus da Caparica, 2829-516, Caparica, Portugal
[c] Comenius University in Bratislava, Mlynská dolina, Ilkovičova 6, SK-842 15, Bratislava, Slovakia
[d] NOVA School of Science and Technology, Department of Earth Sciences, Campus da Caparica, 2829-516, Caparica, Portugal
[e] Eurasia Natural History Association, Ataturk Mah. Lale Cad.11/33, 06909, Ankara, Türkiye
[f] Aker BP ASA, Strandveien 4, Lysaker, 1366, Oslo, Norway

ARTICLE INFO

Keywords:
Artificial intelligence
Machine learning
Dinoflagellate cysts
Palynology
Object detection

ABSTRACT

This study explores the application of YOLOv10, a cutting-edge object detection framework, to automate the identification and classification of *Batioladinium longicornutum*. Utilizing a dataset of 137 annotated images, we trained and validated the model to distinguish *B. longicornutum* from other species with a mean Average Precision (mAP@0.5) of 62.0 %. The methodology incorporated robust data augmentation techniques and evaluation metrics, including precision-recall analysis, confusion matrices, and cross-validation. YOLOv10's architecture facilitated accurate feature extraction and efficient classification, even with a relatively small dataset. While this study focuses on species-level identification, future work will extend to morphological and preservation state classifications, offering broader applications in automated palynology. These findings demonstrate the potential of YOLOv10 to revolutionize taxonomic workflows and enhance the efficiency of paleontological research.

1. Introduction

The rapid advancements in Artificial Intelligence (AI) and Machine Learning (ML) are revolutionizing scientific research across diverse disciplines, including the oil and gas industry (Hoeser and Kuenzer, 2020; Mimura et al., 2023). Geosciences, in particular, are leveraging these technologies to achieve more detailed studies of geological formations, enhancing exploration and production processes (Jensen et al., 1986; Temizel et al., 2021; Li et al., 2023).

Deep learning technologies (Fig. 1) stand out as powerful tools for pattern recognition, data analysis, and predictive modeling (Kumar et al., 2019). Within the petroleum industry, these algorithms are widely employed in tasks such as seismic interpretation, reservoir engineering, and production optimization (Tariq et al., 2021; Hung et al., 2022).

In palynology, the manual identification of species and data analysis are labor-intensive processes that rely on the expertise of highly trained scientists. However, the decline in the number of expert palynologists presents a growing challenge. Automated detection algorithms offer a promising solution to accelerate data analysis and interpretation (Kubera et al., 2021), improving efficiency and accuracy while addressing the expertise gap. Automation facilitates the rapid identification of palynomorphs (Gallardo et al., 2024) and minimizes interpretation errors. Integrating deep learning into palynology has the potential to drive innovation in this field, advancing geological research by increasing the temporal resolution of Earth's history.

The application of these advancements extends to the petroleum industry, where the integration of lithological and paleoenvironmental studies enables faster, more accurate interpretations, complementing expert knowledge without replacing it. Several studies have already demonstrated the effectiveness of deep learning in recognizing microfossils and palynomorphs using a variety of methods (e.g., Carlson et al., 2022; Gonçalves et al., 2022; Gorur et al., 2022; Viertel and König, 2022; Martinsen et al., 2024).

Ozer et al. (2022) introduced a hybrid approach that combines Convolutional Neural Networks (CNNs) with Bidirectional and Long Short-Term Memory (BiLSTM/LSTM) networks to classify the microfossil species Globotruncana, achieving an impressive accuracy of 97.35 %. Carvalho and Aznarte (2019) utilized semantic segmentation for fully

Peer review under the responsibility of KeAi Communications Co., Ltd.
* Corresponding author. Aker BP ASA, Oksenøyveien 10, 1366 Lysaker, Oslo, Norway.
E-mail address: manuel.vieira@akerbp.com (M. Vieira).

https://doi.org/10.1016/j.aiig.2025.100150
Received 10 October 2024; Received in revised form 9 August 2025; Accepted 11 August 2025
Available online 13 August 2025

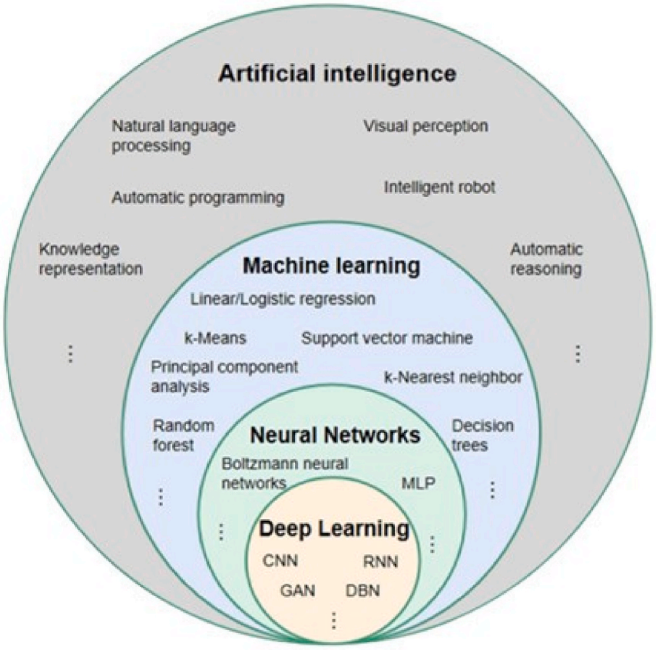

Fig. 1. – Subareas of artificial intelligence (Li et al., 2018).

automated microfossil identification, obtaining a high identification rate of 98 % in drill core samples analyzed with MicroCT. Similarly, Sevillanio and Aznarte (2018) applied three deep learning classification methods to the POLEN23E image dataset, reporting a CNN accuracy of over 97 %. Tetard et al. (2020) developed a workflow for automatic radiolarian image acquisition and identification, achieving approximately 90 % accuracy using a CNN trained on a database of radiolarians from the Neogene to Quaternary periods. Additionally, Zhao et al. (2022) and Martinsen et al. (2024) introduced an automated pollen identification method that integrates localization and classification tasks, simulating the observation process employed by palynologists.

Given the morphological complexity of dinoflagellate cysts, their automatic identification presents a critical challenge, offering the potential to differentiate species and identify unique characteristics that enhance confidence in taxonomic classification.

This study evaluates the application of YOLOv10, a state-of-the-art object detection framework, for the automated detection and recognition of dinoflagellate cysts, using *Batioladinium longicornutum* as a case study. The research focuses on leveraging YOLOv10's advanced architecture to classify this species and its distinct features, enhancing the precision and confidence of identification. The methodology was implemented using the Python programming language and the YOLOv10 repository (https://github.com/THU-MIG/yolov10.git), ensuring robust model performance and scalability for future advancements in automated palynology.

2. Materials and methods

2.1. Sample collection

The focus of this study is on the dinoflagellate cyst species *Batioladinium longicornutum*. Specimens were extracted from well 16/2–21, located in the Norwegian North Sea (Johan Sverdrup oil field), Utsira High area. These specimens have been recovered from core samples taken from an Early Cretaceous (Hauterivian) interval of the Munk Marl Bed, a thick black, laminated, pyritic shaly bed of claystone with algal rich organic matter content (Jasen et al., 1986), part of the regional Åsgard Formation. The specific depth interval of the core samples ranged from 1918 m to 1925 m.

2.2. Sample preparation and imaging

Following collection, the core samples were transported to the Stratum Reservoir core storage facility in Stavanger, Norway, where initial preparation and cataloguing occurred. Subsequent detailed palynological processing and analysis were carried out at the Applied Petroleum Technology (APT) Palynology Laboratory located in Oslo, Norway. This standard laboratory palynology processing included chemical treatment for isolating palynomorphs, mounting on slides, and staining to enhance visibility under microscopy.

2.3. Microscopic analysis and image acquisition

A total of 38 slides containing specimens of *Batioladinium longicornutum* were systematically analyzed using a Nikon Eclipse E600 optical microscope at the NOVA School of Science and Technology, Caparica, Portugal. Each slide was carefully examined to ensure thorough coverage of all observable specimens. High-resolution imaging was performed using the built-in camera of the Nikon Eclipse E600 microscope, with a total of 1453 images captured. The images were cropped and selected based on strict criteria of clarity and morphological representativeness, ensuring that the dataset accurately reflected the defining characteristics of the species. This rigorous selection process aimed to maximize the reliability and quality of subsequent analyses. The overall development process of the detection model is illustrated in Fig. 2.

2.4. Dataset description

The dataset used in this study consisted of 1453 high-resolution images of dinoflagellate cysts. Each image in the dataset contains a single specimen, systematically annotated to capture the morphological features of *Batioladinium longicornutum* and other species. The dataset was divided into three subsets to ensure a balanced and comprehensive training, validation, and testing process:

- Training Set: 137 images, including 68 images of *Batioladinium longicornutum* and 69 images of other species. This subset was used to train the YOLOv10 model, enabling it to learn distinguishing features of the target species while accounting for variability in the non-target species.

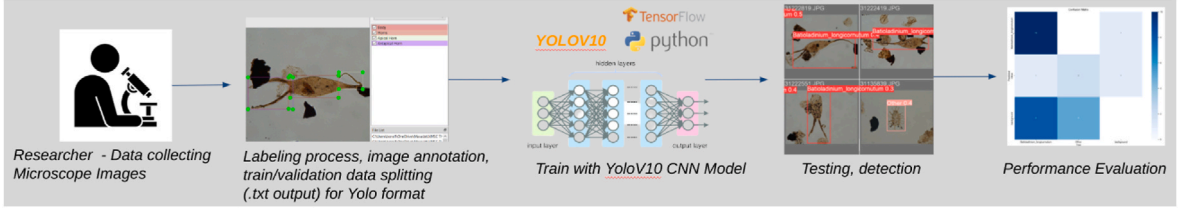

Fig. 2. Development process of the detection model.

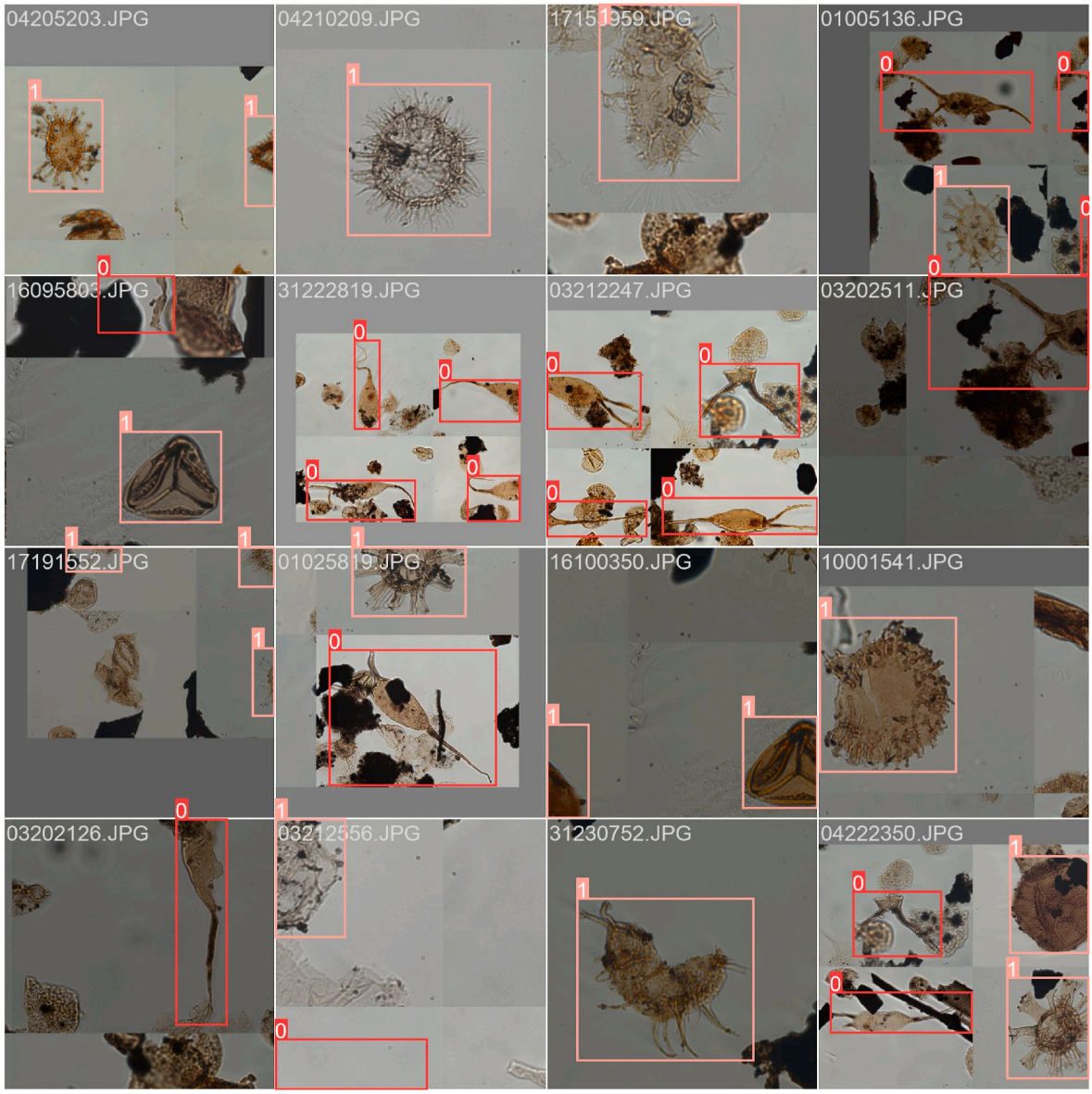

Fig. 3. Visualization of the image annotation process, showing bounding box creation around individual dinoflagellate cysts. Class 0 represents *Batioladinium longicornutum*, and Class 1 represents other species.

- Validation Set: 40 images, with 20 images of *Batioladinium longicornutum* and 20 images of other species. This set was employed to fine-tune the model during training, monitor its performance, and prevent overfitting by ensuring that the model generalized well beyond the training data.
- Test Set: 1316 images, comprising 95 images of *Batioladinium longicornutum* and 1221 images of other species.

The annotation process was conducted manually using LabelImg Python script, and converted to the YOLOv10 format (.txt), a widely adopted open-source image annotation tool. Each image was meticulously reviewed to ensure accuracy, and bounding boxes were drawn around individual cysts to isolate them from the background. This process allowed the creation of annotations that accurately reflected the morphological characteristics of *Batioladinium longicornutum*, including its distinctive morphological features (apical horn and antapical horns) and preservation state. The annotation process evaluation and boxing visualization are shown in Fig. 3.

2.5. YOLOv10 model architecture

The YOLOv10 architecture was selected for this study due to its advanced capabilities in object detection and classification, offering a balance of speed, precision, and scalability.

Backbone: The architecture employs CSPDarkNet53 as its backbone, a highly efficient network designed for hierarchical feature extraction. This backbone utilizes Cross-Stage Partial (CSP) connections to reduce computational overhead while maintaining high accuracy. By effectively capturing both low-level and high-level features, CSPDarkNet53 is particularly suited for tasks involving complex textures and patterns, such as those presented by dinoflagellate cysts.

Neck: A Path Aggregation Network (PAN) is integrated into the architecture to facilitate multi-scale feature fusion. PAN propagates low-level features from earlier layers and combines them with high-level semantic information from deeper layers. This design enhances the model's ability to detect small objects, which is critical for accurately identifying *Batioladinium longicornutum* in microscopic images.

Head: The model's head features a decoupled detection structure,

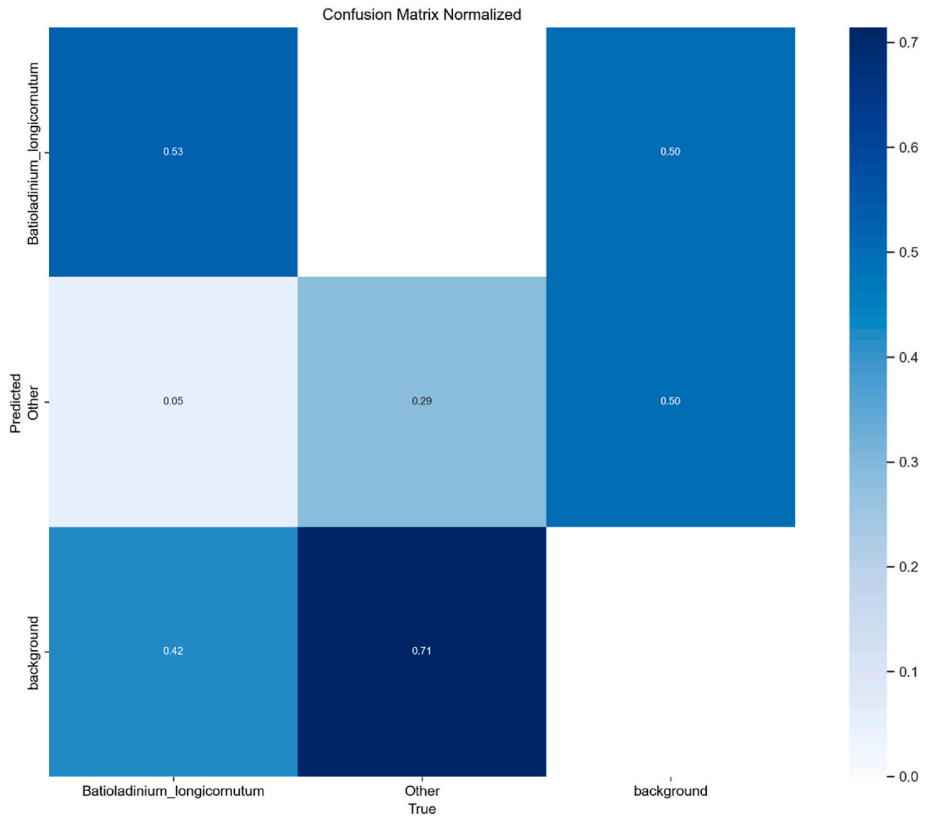

Fig. 4. A normalized confusion matrix illustrating the alignment between the actual class labels (ground truth) and the classifications predicted by the model.

separating bounding box regression from classification tasks. This decoupling allows the model to optimize each task independently, improving both the precision of bounding box predictions and the accuracy of species classification. The head outputs bounding box coordinates, class probabilities, and objectness scores, providing a comprehensive assessment of each detected object.

To process the input data, all images were resized to a uniform resolution of 640 × 640 pixels. This resolution was chosen to strike a balance between computational efficiency and detection accuracy. Resizing ensures consistent input dimensions for the model while preserving sufficient detail for identifying subtle morphological features.

2.6. Training procedure

The training process was implemented using the Python programming language and the YOLOv10 repository, leveraging its robust framework for fine-tuning object detection models. The following parameters and strategies were employed to ensure effective model training and optimization:

- Learning Rate: The initial learning rate was set at 0.001, with a scheduled decay by a factor of 0.1 every 500 steps. This gradual reduction in the learning rate allowed the model to make significant updates during early training while fine-tuning parameters during later stages to converge effectively.
- Batch Size: A batch size of 16 was chosen, balancing computational efficiency and the ability to process diverse samples within each iteration. This size ensured that the model could effectively learn from both *Batioladinium longicornutum* and other species in each batch.
- Epochs: The training process was conducted over 200 epochs, allowing the model sufficient iterations to learn complex patterns and features within the dataset. The number of epochs was optimized to prevent overfitting while ensuring the model achieved stable performance on the validation set.

Data Augmentation: To enhance the robustness and generalization of the model, advanced data augmentation techniques were applied.

- Mosaic Augmentation: Combined four images into a single input, creating diverse spatial contexts and improving the model's ability to generalize across varying object placements.
- Mixup: Blended two images and their corresponding annotations, introducing variability in image content and reducing overfitting.
- Random Rotations: Applied rotations within a range of $\pm 15^{\circ}$ to simulate different orientations of the specimens.
- Horizontal Flips: Reversed images horizontally to increase diversity and simulate realistic variations in image capture.
- Brightness and Contrast Adjustments: Slight alterations in brightness and contrast were introduced to account for variations in lighting conditions during image acquisition.

2.7. Evaluation metrics

The performance of the YOLOv10 model was comprehensively evaluated using a range of metrics designed to capture different aspects of detection and classification accuracy. These metrics included:

- Precision (π): Measures the proportion of correctly predicted positive cases out of all predicted positive cases.
- Recall (ρ): Measures the proportion of correctly predicted positive cases out of all actual positive cases.
- F1-Score: Combines precision and recall into a single metric, providing a harmonic mean.

These metrics provide insight into the model's ability to balance true

Fig. 5. Example of validation prediction.

positives, false positives, and false negatives, critical for accurate classification of *Batioladinium longicornutum*.

- Confusion Matrices: Raw and normalized confusion matrices were generated to visualize the distribution of predictions across classes. The confusion matrix included True Positives (TP), False Positives (FP), True Negatives (TN), and False Negatives (FN) for each class, allowing a detailed analysis of misclassifications and overall classification performance.
- Mean Average Precision (mAP): Evaluates the model's Average Precision (AP) at an Intersection over Union (IoU) threshold of 0.5. The AP for each class is computed as the area under the Precision-Recall curve, and the mean of these AP values across all classes gives the mAP.

3. Preliminary results

The performance of the YOLOv10 model was evaluated using the test dataset of 1316 images, consisting of 95 images of *Batioladinium longicornutum* and 1221 images of other species. The results are presented below, based on key evaluation metrics and visual analyses of the model's performance.

The results show a precision of 68 % in identifying this target species and a lower precision of 56.1 % in identifying other species. The overall performance of the model across all classes, as an average precision (mAP@0.5) of 62.0 %.

3.1. Confusion matrix analysis

This section presents a comprehensive analysis of the YOLOv10 model's performance, initially focusing on the validation set for hyperparameter tuning and monitoring training loss, and subsequently extending to the test set to reflect the model's generalization capabilities. While the validation set was crucial for iterative model refinement and preventing overfitting during training, the test set provides an unbiased evaluation of the model's performance on unseen data. The potential impact of class imbalance on the test set results, particularly concerning precision and recall for different classes, is also discussed.

The normalized confusion matrix insights into the classification accuracy. Most misclassifications occurred between classes and

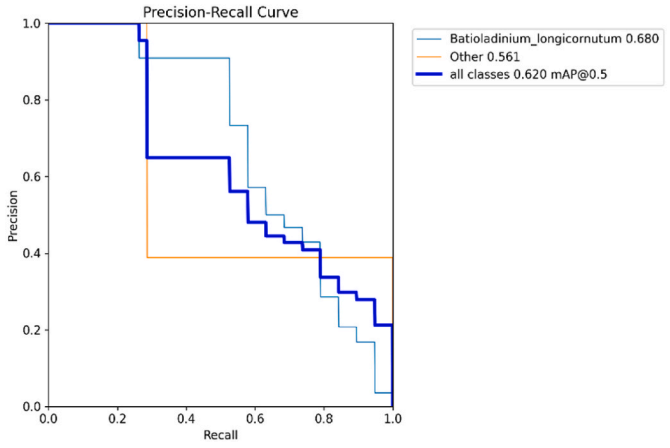

Fig. 6. Precision-Recall Curve, illustrating the trade-off between precision and recall for the YOLOv10 model across various confidence thresholds. This curve is essential for understanding the model's performance at different operating points.

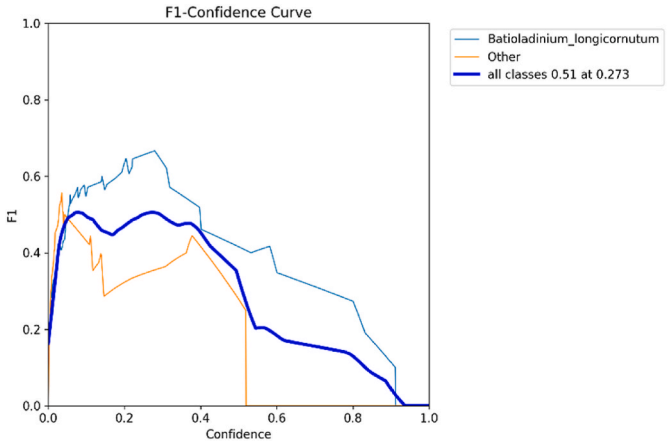

Fig. 7. F1-Confidence Curve, showing the F1-score at different confidence thresholds. The optimal balance between precision and recall for all classes was achieved at a confidence threshold of 0.27, as indicated by the peak of the curve.

background. Background typically refers to areas within the image that do not contain any of the classes being detected (*Batioladinium longicornutum* or "Other species"). It represents all pixels or regions where no object of interest was identified and serves as a control category in object detection models. False Positives for Background or Off-diagonal values (e.g., 0.42 for "background" predicted as *Batioladinium longicornutum*) indicate misclassifications where the model mistakenly labeled a background region as a target class (Fig. 4).

For the test set, the results show a precision of 68 % in identifying *Batioladinium longicornutum* and a lower precision of 56.1 % in identifying other species. The overall performance of the model across all classes, as an average precision (mAP@0.5) of 62.0 %.

Fig. 5 shows and example of model prediction for validation set.

3.2. Visual performance analysis

To further elucidate the YOLOv10 model's behavior and performance beyond quantitative metrics, a visual analysis of key performance indicators was conducted. This section provides insights into the model's detection and classification capabilities through graphical representations, showcasing its strengths, identifying areas for improvement, and offering a more intuitive understanding of its operational

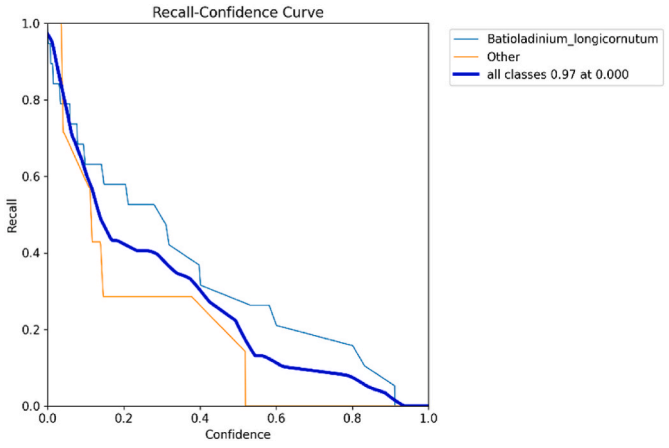

Fig. 8. Recall-Confidence Curve, illustrating the relationship between recall and confidence thresholds. This curve demonstrates how recall changes as the model's confidence in its predictions varies.

characteristics. The following visualizations detail various aspects of the model's performance:

- Precision-Recall Curve: Demonstrates the trade-offs between precision and recall across confidence thresholds (Fig. 6). The model achieved an optimal balance at a confidence threshold of 0.27 (Fig. 7).
- Recall-Confidence Curve: Shows diminishing recall with increasing confidence thresholds, reflecting the model's sensitivity to classification thresholds (Fig. 8). In these figures, "confidence" refers to the softmax output for each class, representing the model's certainty that a detected object belongs to a particular class. The maximum confidence value is typically used as the class prediction, as it indicates the most probable class assigned by the model. Training Metrics: Plots of bounding box loss and classification loss over 200 epochs show steady convergence, indicating effective training (Fig. 9).

3.3. Challenges and limitations

While the YOLOv10 model demonstrated strong performance in detecting and classifying *Batioladinium longicornutum*, our initial evaluation relied primarily on the validation dataset. This approach is standard in model development, as the validation set is used for hyperparameter tuning and to mitigate overfitting. In line with the default YOLOv10 pipeline, which performs automatic evaluation on the validation set, no separate test set was included by default and would need to be specified manually. Therefore, in this study we adhered to the standard YOLOv10 framework, using the validation set as the primary basis for performance assessment given the study's scope and constraints.

However, this approach revealed several challenges that impacted its effectiveness, particularly when considering real-world application and the model's generalization capabilities on truly unseen data. Preliminary observations of the available independent test set indicated a heavily skewed class distribution, with a significantly larger number of images of individual specimens representing other species (1221 images) compared to *Batioladinium longicornutum* (95 images). This pronounced class imbalance likely affected the model's recall for the target species, as it encountered fewer representative examples during training to generalize effectively. Dataset imbalance is a common issue in deep learning applications and can lead to biased predictions, where the model becomes more attuned to the majority class, potentially overestimating performance on minority classes when evaluated on a representative test set.

These preliminary findings, derived from both validation outcomes

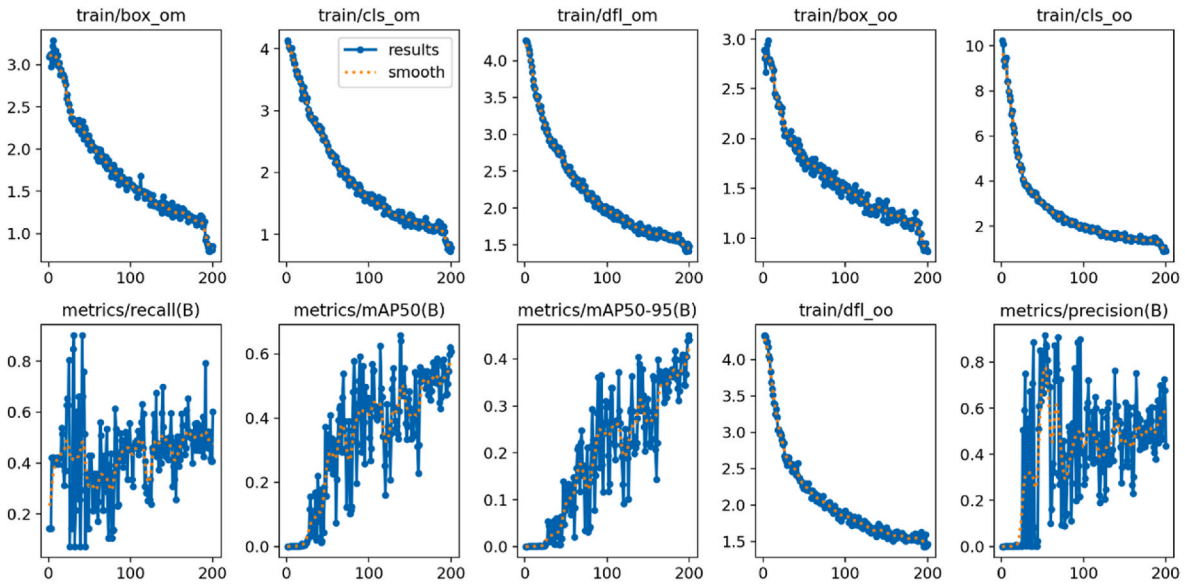

Fig. 9. The curves display loss (box_loss, cls_loss, dfl_loss) for the YOLOv10 model during training. The metrics/mAP50-95(B) represents the mean Average Precision (mAP) calculated over multiple Intersection over Union (IoU) thresholds, ranging from 0.50 to 0.95, with a step size of 0.05. This metric provides a comprehensive evaluation of the model's detection accuracy across various levels of localization precision.

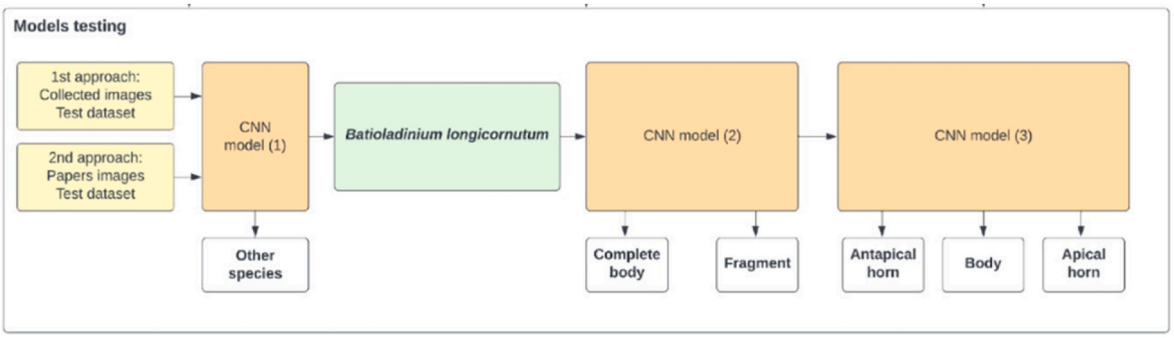

Fig. 10. – Model testing algorithm diagram for future aspect.

and an understanding of the test set's characteristics, emphasize the robustness and potential of the YOLOv10 model for automated palynological analyses. At the same time, they underscore the importance of addressing dataset limitations and ensuring proper generalization on unseen data. Future work will focus on mitigating these challenges by expanding the dataset, incorporating additional classes, and performing comprehensive evaluation on a dedicated and balanced test set.

4. Applications beyond species identification

The developed methodology demonstrates significant potential for applications beyond the initial scope of species identification, particularly in the classification of preservation states and detailed morphological features of *Batioladinium longicornutum*.

One application of this methodology focuses on evaluating the preservation quality of *Batioladinium longicornutum* cysts. Using a specialized dataset, the model categorizes cysts into two classes:

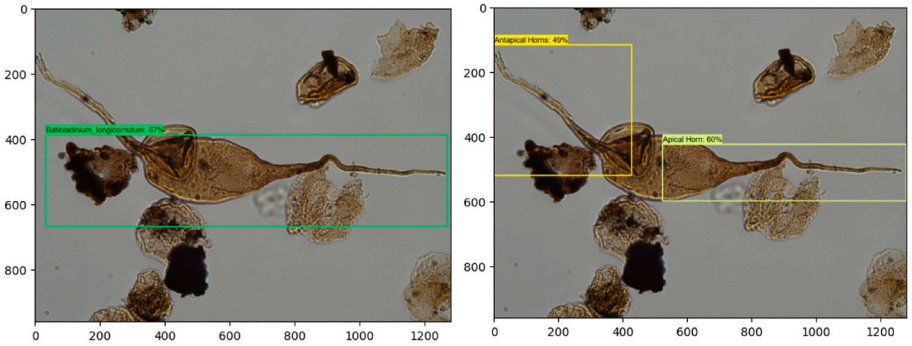

Fig. 11. Ilustration of specific features identification.

"Complete body" and "Fragmented body." These classifications provide crucial insights into the structural integrity of the specimens, which are vital for paleoenvironmental and diagenetic studies. By distinguishing between intact and damaged cysts, the model supports more accurate reconstructions of paleoenvironmental conditions and assessments of diagenetic alterations (Fig. 10).

Another application involves the detailed characterization of specific morphological features of *Batioladinium longicornutum*. The model was trained on a dataset with classifications for "Antapical horn," "Apical horn," and "Body." This targeted analysis enables the identification of intricate morphological details that are critical for understanding the variability and evolutionary significance of these features. Such detailed classifications can also facilitate the differentiation of similar species within complex datasets, advancing the field of automated taxonomy.

A potential application of a multi-model framework approach highlighting several notable capabilities and challenges: incomplete species detection and specific species features identification.

Fig. 11 shows an example of potential application of feature identification, using a TensorFlow implementation of the pre-trained model SSD MobileNet V2 FPNLite 320x320 (Chiu et al., 2020).

5. Discussion

The results of this study underscore the efficacy of YOLOv10 in automating the detection and classification of *Batioladinium longicornutum*, offering promising implications for the field of palynology. Despite the inherent challenges posed by dataset imbalance and the morphological complexity of dinoflagellate cysts, the model achieved a mean Average Precision (mAP@0.5) of 62.0 %, highlighting its potential as a robust tool for taxonomic workflows.

The YOLOv10 model demonstrated a commendable ability to identify *Batioladinium longicornutum*, achieving a precision of 68 % for this target species. While lower precision (56.1 %) was observed for other species, the overall results affirm the model's capacity to distinguish between complex morphological species. The confusion matrix analysis revealed notable misclassifications, particularly with the background category, which highlights the sensitivity of the model to non-target regions in images. This issue aligns with challenges reported in similar studies where object detection models struggled with distinguishing fine details amidst noisy backgrounds.

The primary limitation of this study was the dataset imbalance, with significantly fewer images of *Batioladinium longicornutum* compared to other species. This disparity likely influenced the model's ability to generalize for the target species, as the limited representation of *B. longicornutum* in the training set constrained its learning potential. Additionally, the high variability in morphological features within the dataset presented a challenge for accurate classification, particularly for specimens in different preservation states or orientations.

The model's reliance on high-resolution images and manual annotations further underscores the need for scalable approaches in automated palynology. While YOLOv10 performed well within the defined parameters, its precision could be enhanced by incorporating larger and more diverse datasets. Future studies should explore methods to address dataset imbalance, such as synthetic data generation or transfer learning, to improve model robustness and accuracy.

Future work will focus on extending the capabilities of YOLOv10 to classify preservation states and detailed morphological features of dinoflagellate cysts. Incorporating additional classes and refining the annotation process can enhance the model's ability to capture subtle variations in cyst morphology. The development of hybrid models, combining convolutional and recurrent neural network architectures, could further improve the precision and recall metrics, particularly for underrepresented classes.

6. Conclusion

This study underscores the potential of YOLOv10 as an advanced tool for automating the identification and classification of dinoflagellate cysts, addressing a critical need in palynology. The results demonstrate the model's capability to handle complex morphological structures, making it a promising addition to taxonomic workflows. However, challenges such as dataset imbalance and the inherent variability in cyst morphology highlight the need for further refinements. By expanding the dataset to include more diverse and representative samples, future research can improve the model's ability to generalize across underrepresented and morphologically complex species. Incorporating advanced techniques, such as synthetic data generation, transfer learning, and hybrid model architectures, can further enhance detection accuracy and classification performance.

These advancements would solidify the model's role in automating palynological analyses, accelerating species identification, and reducing reliance on manual methods. Ultimately, this progress will open new avenues for studying Earth's paleoenvironmental history with greater precision and efficiency, contributing valuable insights into past climates and ecosystems.

CRediT authorship contribution statement

A. Sanches: Writing – review & editing, Writing – original draft, Project administration, Methodology, Investigation, Formal analysis, Conceptualization. **B. Ağbulut:** Writing – original draft, Methodology, Formal analysis. **L. Castro:** Writing – review & editing, Writing – original draft, Supervision, Conceptualization. **M. Vieira:** Writing – review & editing, Writing – original draft, Supervision, Conceptualization.

Declaration of competing interest

The authors declare that they have no known competing financial interests or personal relationships that could have appeared to influence the work reported in this paper.

Acknowledgments

We thank AkerBP for their generous provision of the core samples that made this study possible. We also thank the reviewers for their constructive feedback, which helped improve the clarity and quality of this paper.

References

Carlson, E.A., Smith, J.R., Smith, J.R., 2022. Convolutional neural networks for microfossil recognition in sediment samples. Mar. Micropaleontol. 111, 1015421.

Carvalho, L.M., Aznarte, J.L., 2019. Automated microfossil identification using semantic segmentation and MicroCT data. J. Paleont. Techniq 12 (3), 98–1121.

Chiu, Y.-C., Tsai, C.-Y., Ruan, M.-D., Shen, G.-Y., Lee, T.-T., 2020. Mobilenet-SSDv2: an improved object detection model for embedded systems. 2020 International Conference on System Science and Engineering (ICSSE). Kagawa, Japan, pp. 1–5. https://doi.org/10.1109/ICSSE50014.2020.9219319.

Gallardo, J.C., Rodriguez, J.A., Rodriguez, J.A., 2024. Automated palynomorph identification using deep learning techniques. Palaeogeogr. Palaeoclimatol. Palaeoecol. 110, 1106821.

Gonçalves, L.M., Silva, R.C., Silva, R.C., 2022. Deep learning-based palynomorph classification using transfer learning. Palynology 46, 1–151.

Gorur, S., Yilmaz, E., Yilmaz, E., 2022. Application of recurrent neural networks for palynological data analysis. Palaeogeogr. Palaeoclimatol. Palaeoecol. 110, 1106821.

Hoeser, T., Kuenzer, C., 2020. Artificial intelligence and machine learning in remote sensing for natural hazard monitoring and disaster management. Remote Sens. 12, 6581.

Hung, N.Q., Nguyen, T.T., Nguyen, T.T., 2022. Deep learning-based production optimization in oil reservoirs. J. Petrol. Sci. Eng. 204, 1086821.

Jensen, T.F., Holm, L., Frandsen, N., Michelsen, O., 1986. Jurassic-lower cretaceous lithostratigraphic nomenclature for the Danish central trough. Danmarks Geol. Underssogelse 12 (Series A), 7–65.

Kubera, E., Kubik-Komar, A., Piotrowska-Weryszko, K., Skrzypiec, M., 2021. Deep learning methods for improving pollen monitoring. Sensors 21, 3526. https://doi.org/10.3390/s21103526.

Kumar, V., Rajan, B., Venkatesan, R., Lecinski, J., 2019. Understanding the role of artificial intelligence in personalized engagement marketing. Calif. Manag. Rev. 61, 135–155. https://doi.org/10.1177/0008125619859317.
Li, Y., Wang, X., Wang, X., 2018. Comparative study of deep learning models for object detection. In: Computer Vision and Image Understanding, 120, 1106821.
Li, Y., Zhang, Y., Wang, Y., 2023. Deep learning-based seismic facies classification for reservoir characterization. J. Appl. Geophys. 197, 1050001.
Martinsen, I., Wade, D., Ricaud, B., Godtliebsen, F., 2024. The 3-billion fossil question: how to automate classification of microfossils. Artificial Intell. Geosci. 5, 100080. https://doi.org/10.1016/j.aiig.2024.100080.
Mimura, N., Yasuhara, K., Yokota, S., 2023. Machine learning-based prediction of earthquake-induced landslides using remote sensing data. Nat. Hazards 107, 1–181.
Ozer, A., Demir, M., Demir, M., 2022. Hybrid CNN-LSTM method for automated palynomorph recognition. Palynology 46, 1–15.
Sevillanio, R., Aznarte, J.L., 2018. Deep learning classification methods for palynological image datasets. Palynology 45 (2), 97–1101.
Tariq, M.A., Al-Mudhafar, W.A., Al-Mudhafar, W.A., 2021. Deep learning-based reservoir characterization using well logs and seismic data. J. Petrol. Sci. Eng. 204, 1086821.
Temizel, A., Kucukdemirci, M., Kucukdemirci, M., 2021. A review of artificial intelligence applications in petroleum geology. J. Petrol. Sci. Eng. 204, 1086821.
Tetard, J., Smith, A.B., Smith, A.B., 2020. Automatic radiolarian image acquisition and identification using convolutional neural networks. Mar. Micropaleontol. 115, 1015421.
Viertel, T., König, M., 2022. Hybrid deep learning approach for palynomorph identification. Mar. Micropaleontol. 111, 1015421.
Zhao, Y., Wang, X., Wang, X., 2022. Simulation-based automatic pollen identification for pollinosis prevention. Palaeogeogr. Palaeoclimatol. Palaeoecol. 120, 1106821.